

SUPPORTING INFORMATION

Facile synthesis of Cu catalysts with multiple high-index facets for the suppression of competing H₂ evolution during the electrocatalytic CO₂ reduction

Monday Philip,^{a,b} Abebe Reda Woldu,^{a,b,c*} Bilal Akbar,^{a,b} Hitler Louis,^{a,b} Huang Cong,^{a,b}

^aCAS Laboratory of Nanosystem and Hierarchical Fabrication, CAS Center for Excellence in Nanoscience, National Center for Nanoscience and Technology, Beijing 100190, China.

^bUniversity of Chinese Academy of Sciences, Beijing 100049, China.

^cDepartment of chemistry, college of science, Bahir Dar University, Bahir Dar 79, Ethiopia.

*Corresponding Author: abebe.reda2@gmail.com

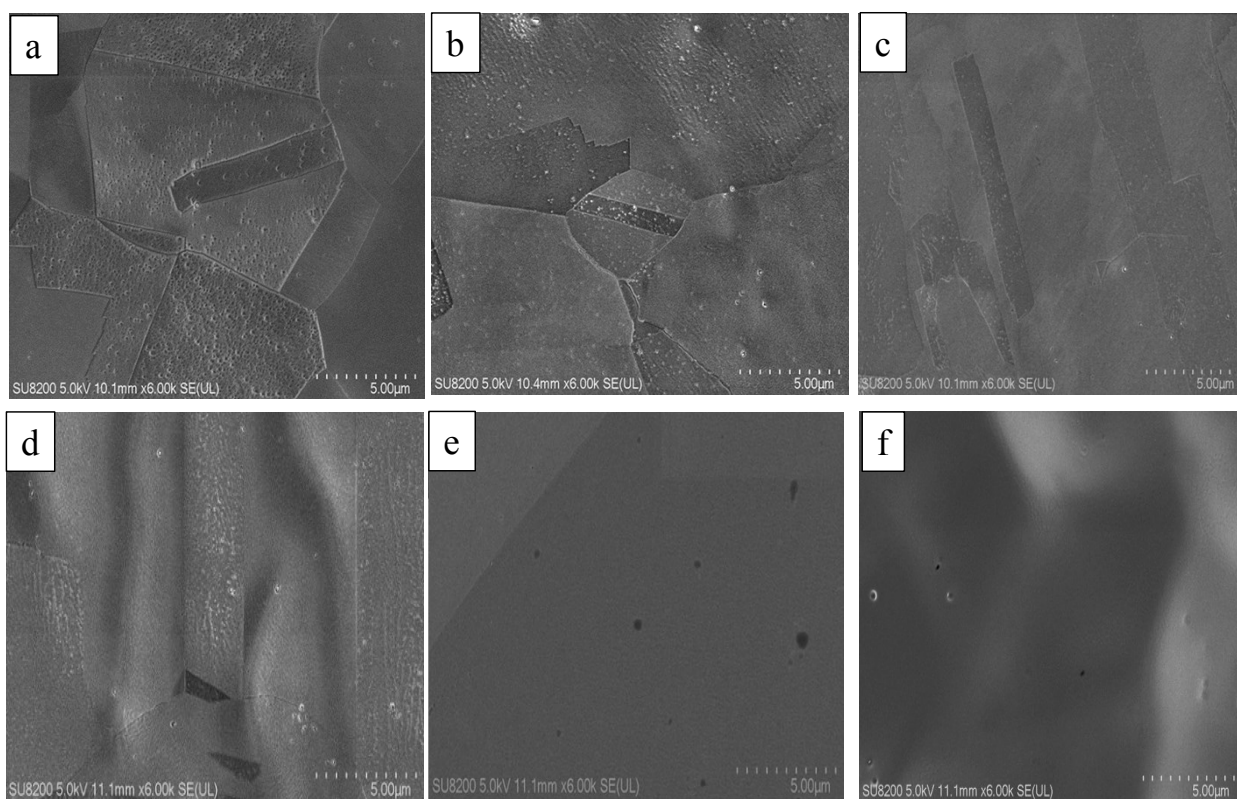


Fig. S1 SEM images of different electrodes before CO₂RR, a) P-Cu, b) P-Cu-200, c) P-Cu-400, d) P-Cu-600, e) P-Cu-800, and f) P-Cu-1000. Scale bar: 5.0 μm.

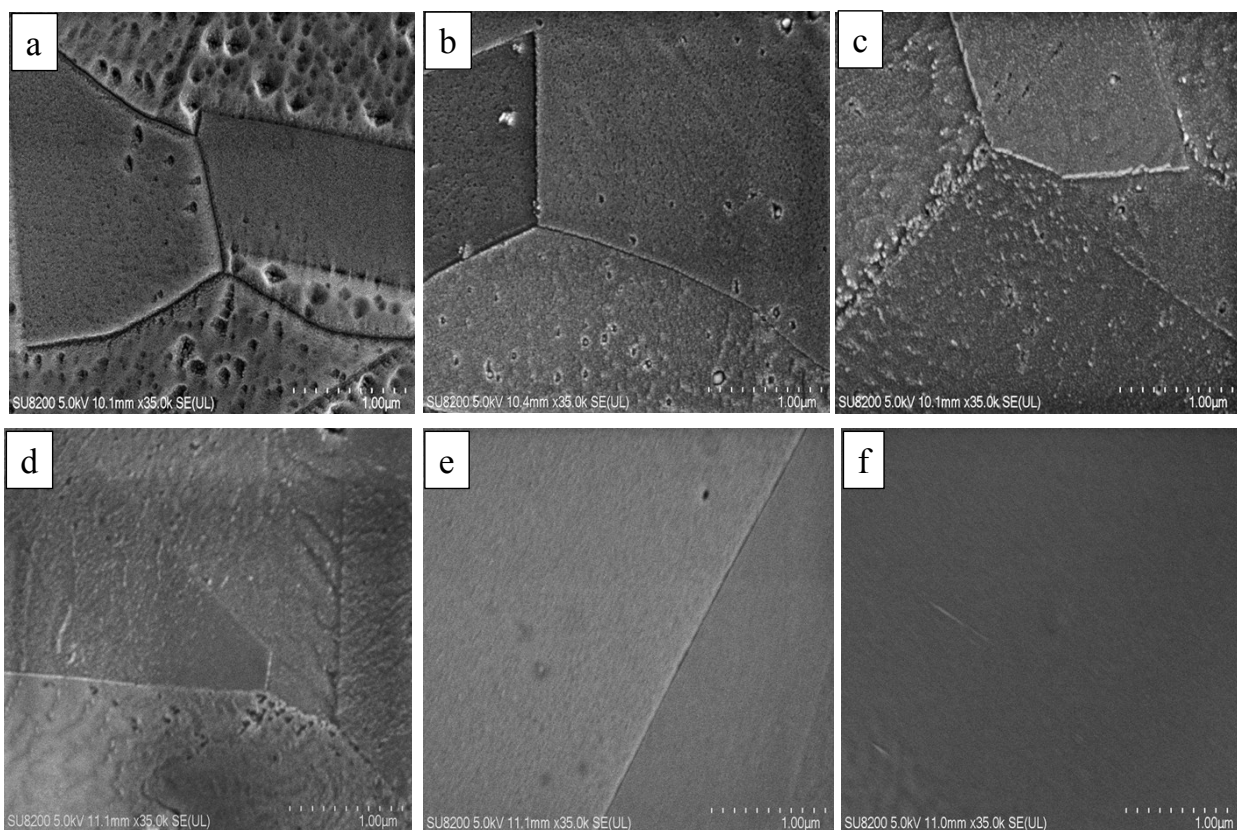
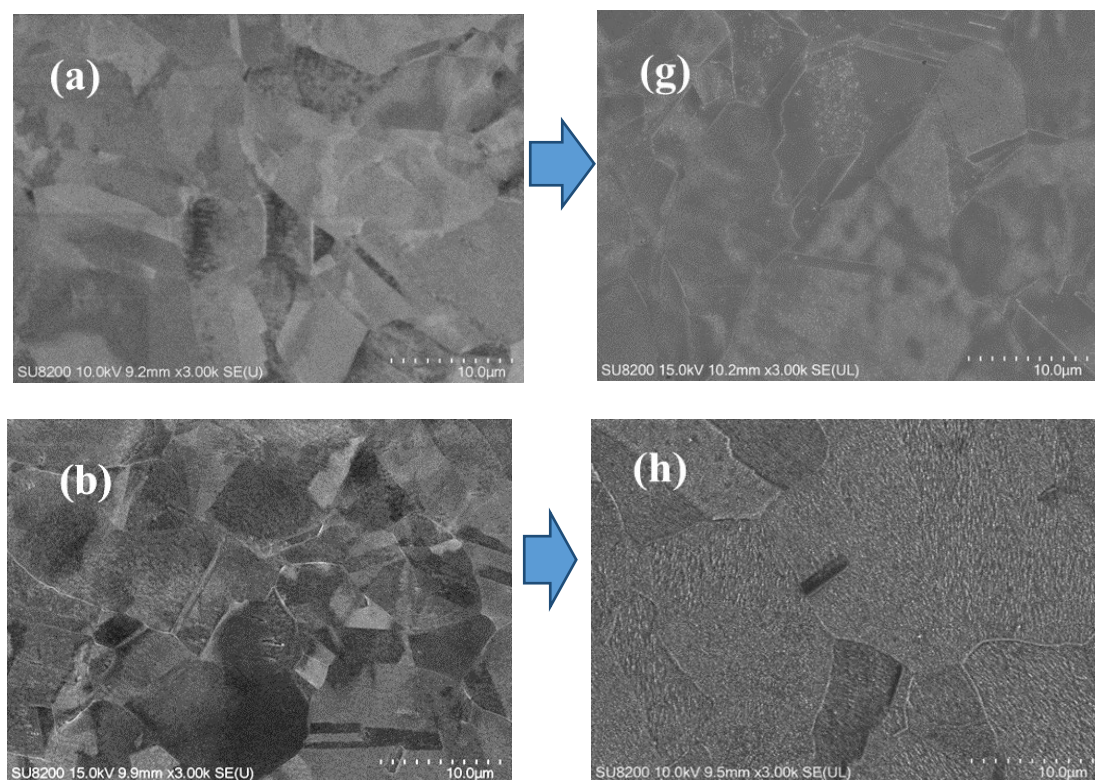


Fig. S2 Additional SEM images of different electrodes before CO₂RR, a) P-Cu, b) P-Cu-200, c) P-Cu-400, d) P-Cu-600, e) P-Cu-800, and f) P-Cu-1000. Scale bar: 1.0 μm.



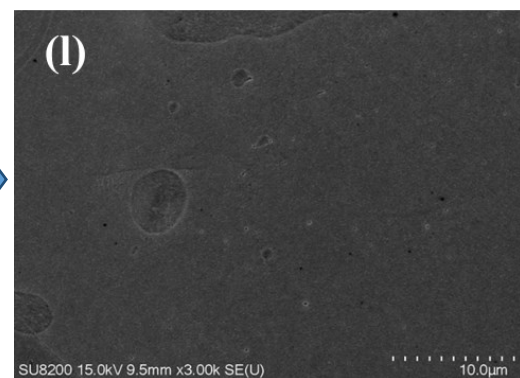
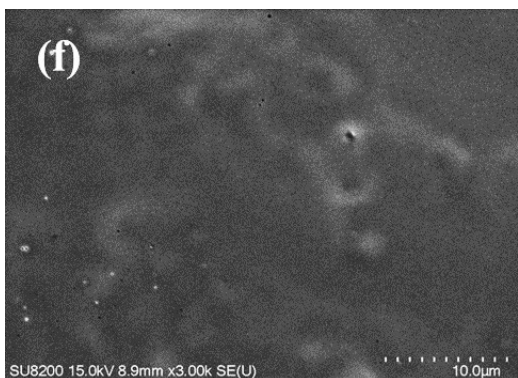
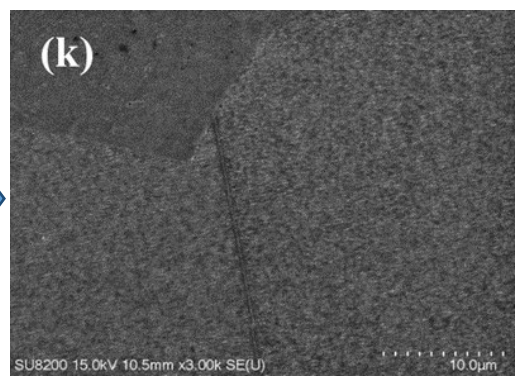
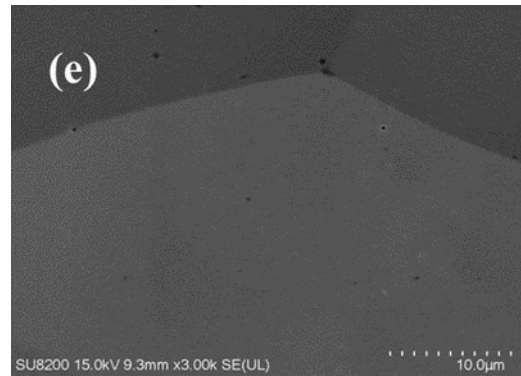
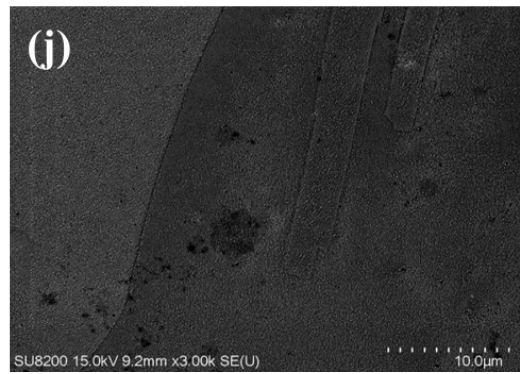
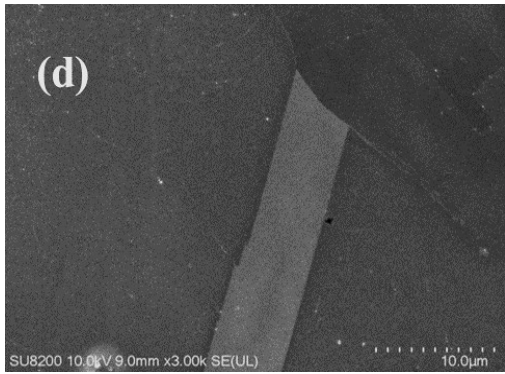
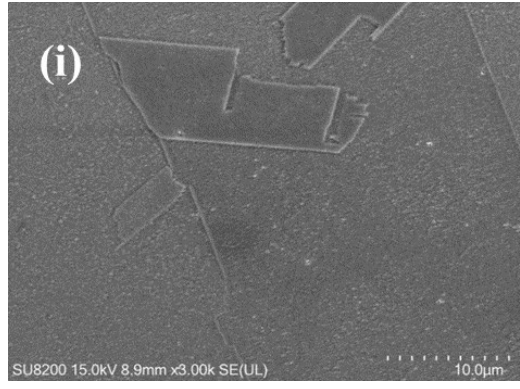
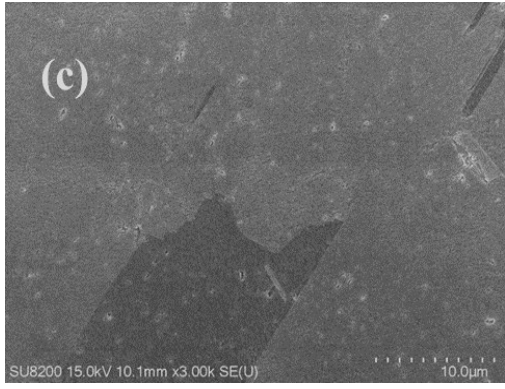
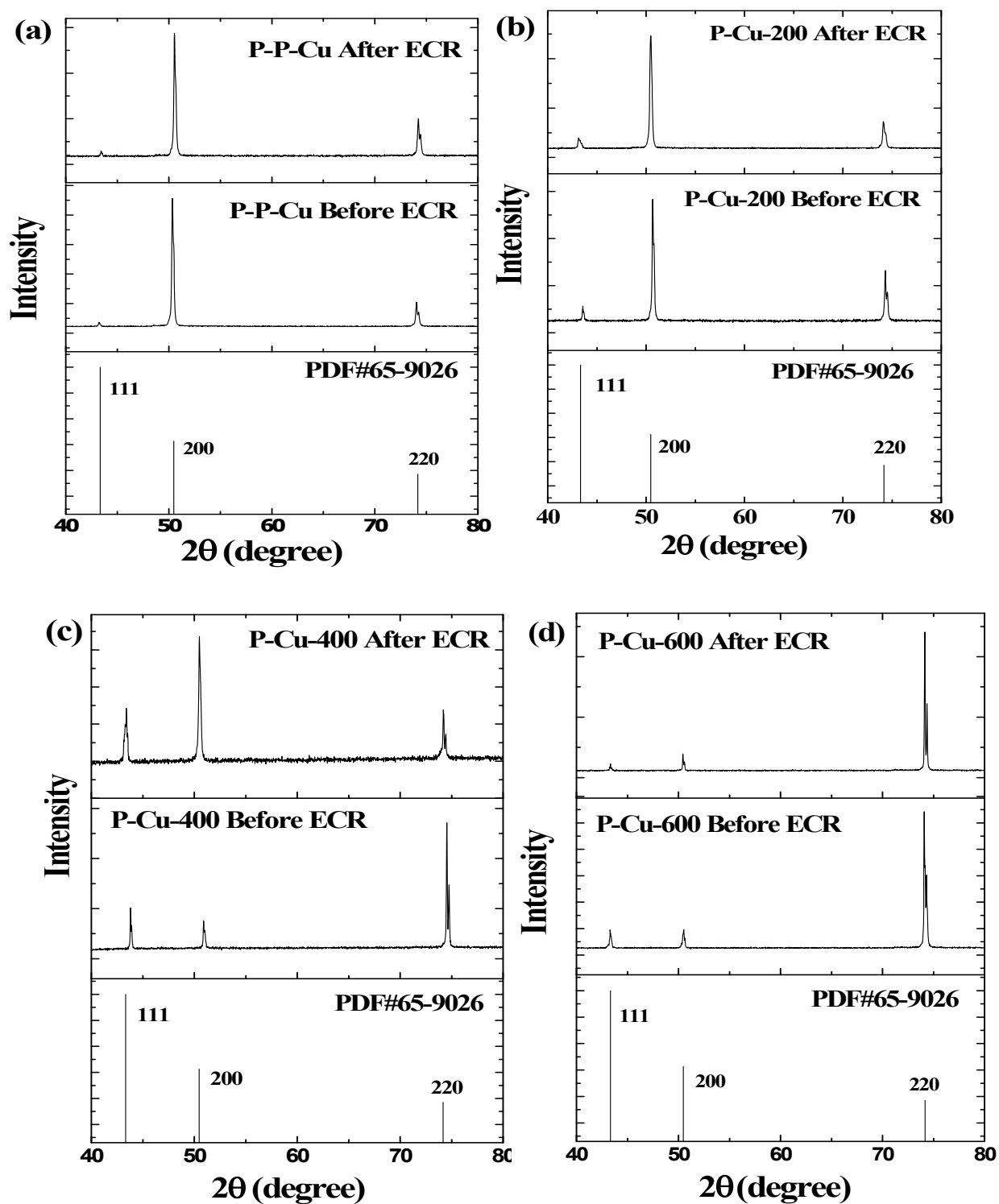


Fig. S3 SEM images of different electrodes before CO₂RR, a) P-Cu, b) P-Cu-200, c) P-Cu-400, d) P-Cu-600, e) P-Cu-800, f) P-Cu-1000; and after CO₂RR, g) P-Cu, h) P-Cu-200, i) P-Cu-400, j) P-Cu-600, k) P-Cu-800, and l) P-Cu-1000. Scale bar: 10.0 μm .



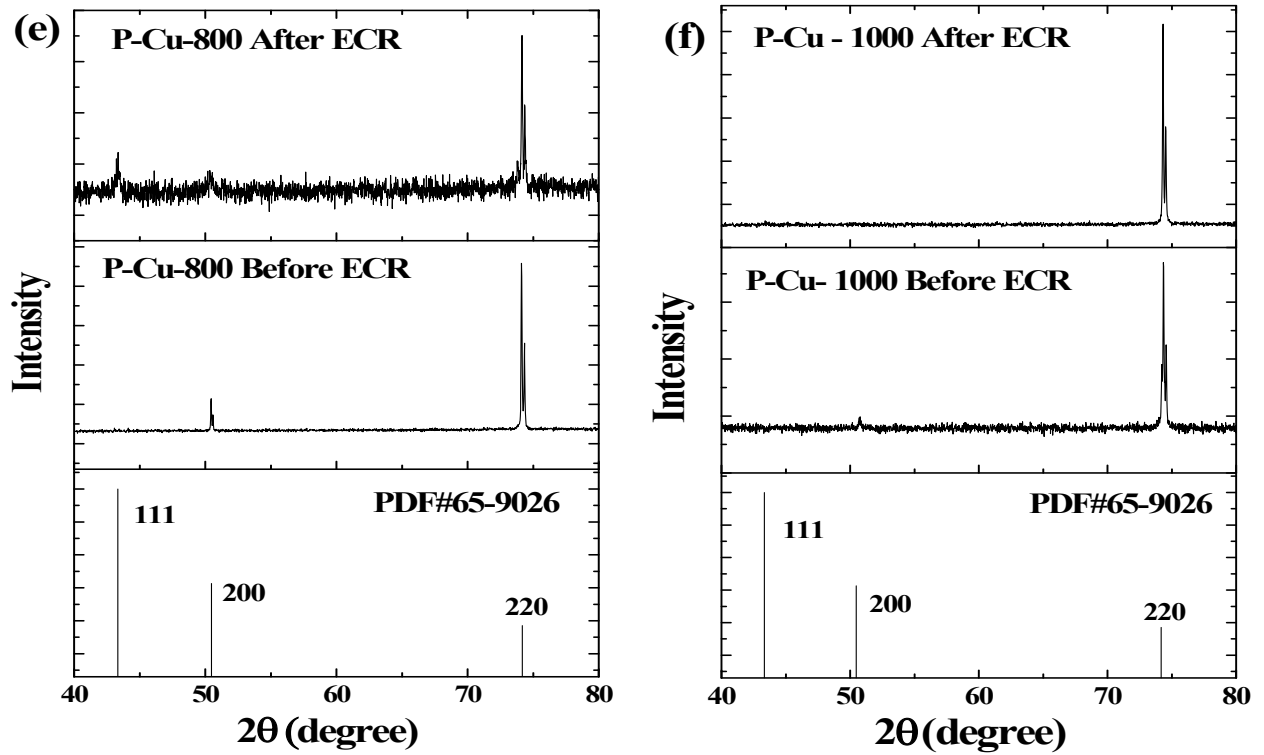
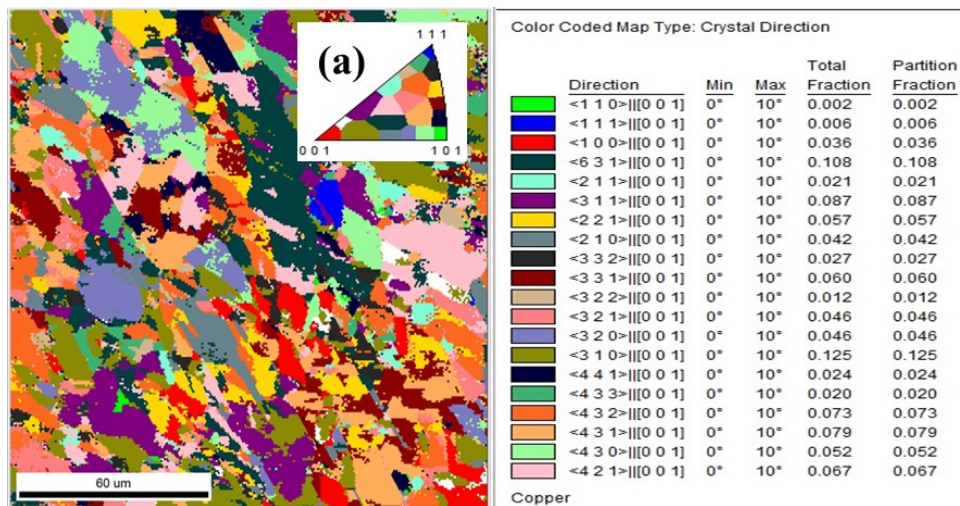
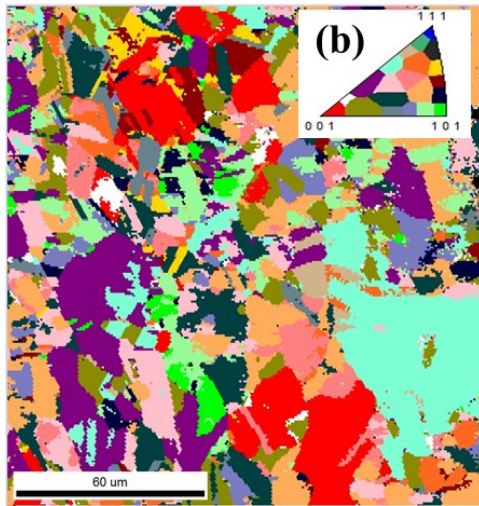


Fig. S4 XRD patterns of different electrodes before and after ECR. (a) P-P-Cu, (b) P-Cu-200, (c) P-Cu-400, (d) P-Cu-600, (e) P-Cu-800, and (f) P-Cu-1000.

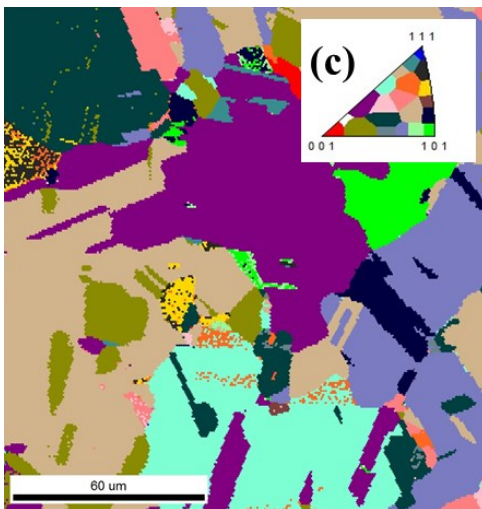




Color Coded Map Type: Crystal Direction

Direction	Min	Max	Total Fraction	Partition Fraction
<1 1 0> [0 0 1]	0°	10°	0.020	0.020
<1 1 1> [0 0 1]	0°	10°	0.000	0.000
<1 0 0> [0 0 1]	0°	10°	0.088	0.088
<6 3 1> [0 0 1]	0°	10°	0.085	0.085
<2 1 1> [0 0 1]	0°	10°	0.115	0.115
<3 1 1> [0 0 1]	0°	10°	0.107	0.107
<2 2 1> [0 0 1]	0°	10°	0.013	0.013
<2 1 0> [0 0 1]	0°	10°	0.022	0.022
<3 3 2> [0 0 1]	0°	10°	0.002	0.002
<3 3 1> [0 0 1]	0°	10°	0.021	0.021
<3 2 2> [0 0 1]	0°	10°	0.012	0.012
<3 2 1> [0 0 1]	0°	10°	0.050	0.050
<3 2 0> [0 0 1]	0°	10°	0.048	0.048
<3 1 0> [0 0 1]	0°	10°	0.078	0.078
<4 4 1> [0 0 1]	0°	10°	0.023	0.023
<4 3 3> [0 0 1]	0°	10°	0.001	0.001
<4 3 2> [0 0 1]	0°	10°	0.030	0.030
<4 3 1> [0 0 1]	0°	10°	0.129	0.129
<4 3 0> [0 0 1]	0°	10°	0.058	0.058
<4 2 1> [0 0 1]	0°	10°	0.087	0.087

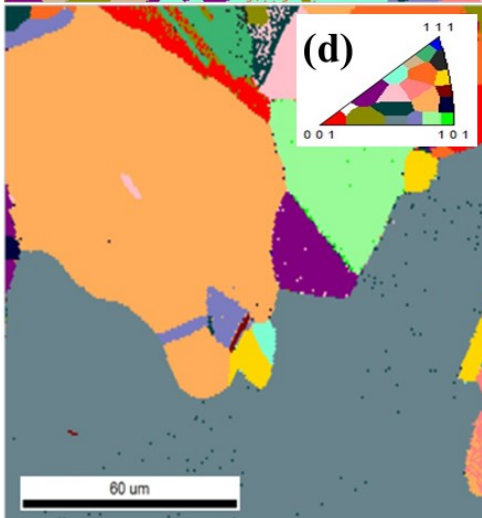
Copper



Color Coded Map Type: Crystal Direction

Direction	Min	Max	Total Fraction	Partition Fraction
<1 1 0> [0 0 1]	0°	10°	0.033	0.033
<1 1 1> [0 0 1]	0°	10°	0.000	0.000
<1 0 0> [0 0 1]	0°	10°	0.003	0.003
<6 3 1> [0 0 1]	0°	10°	0.102	0.102
<2 1 1> [0 0 1]	0°	10°	0.112	0.112
<3 1 1> [0 0 1]	0°	10°	0.198	0.198
<2 2 1> [0 0 1]	0°	10°	0.008	0.008
<2 1 0> [0 0 1]	0°	10°	0.002	0.002
<3 3 2> [0 0 1]	0°	10°	0.008	0.008
<3 3 1> [0 0 1]	0°	10°	0.001	0.001
<3 2 2> [0 0 1]	0°	10°	0.136	0.136
<3 2 1> [0 0 1]	0°	10°	0.018	0.018
<3 2 0> [0 0 1]	0°	10°	0.133	0.133
<3 1 0> [0 0 1]	0°	10°	0.082	0.082
<4 4 1> [0 0 1]	0°	10°	0.025	0.025
<4 3 3> [0 0 1]	0°	10°	0.005	0.005
<4 3 2> [0 0 1]	0°	10°	0.009	0.009
<4 3 1> [0 0 1]	0°	10°	0.117	0.117
<4 3 0> [0 0 1]	0°	10°	0.006	0.006
<4 2 1> [0 0 1]	0°	10°	0.003	0.003

Copper



Color Coded Map Type: Crystal Direction

Direction	Min	Max	Total Fraction	Partition Fraction
<1 1 0> [0 0 1]	0°	10°	0.003	0.003
<1 1 1> [0 0 1]	0°	10°	0.000	0.000
<1 0 0> [0 0 1]	0°	10°	0.029	0.029
<6 3 1> [0 0 1]	0°	10°	0.011	0.011
<2 1 1> [0 0 1]	0°	10°	0.002	0.002
<3 1 1> [0 0 1]	0°	10°	0.027	0.027
<2 2 1> [0 0 1]	0°	10°	0.013	0.013
<2 1 0> [0 0 1]	0°	10°	0.528	0.528
<3 3 2> [0 0 1]	0°	10°	0.001	0.001
<3 3 1> [0 0 1]	0°	10°	0.001	0.001
<3 2 2> [0 0 1]	0°	10°	0.000	0.000
<3 2 1> [0 0 1]	0°	10°	0.005	0.005
<3 2 0> [0 0 1]	0°	10°	0.012	0.012
<3 1 0> [0 0 1]	0°	10°	0.007	0.007
<4 4 1> [0 0 1]	0°	10°	0.004	0.004
<4 3 3> [0 0 1]	0°	10°	0.012	0.012
<4 3 2> [0 0 1]	0°	10°	0.029	0.029
<4 3 1> [0 0 1]	0°	10°	0.243	0.243
<4 3 0> [0 0 1]	0°	10°	0.057	0.057
<4 2 1> [0 0 1]	0°	10°	0.017	0.017

Copper

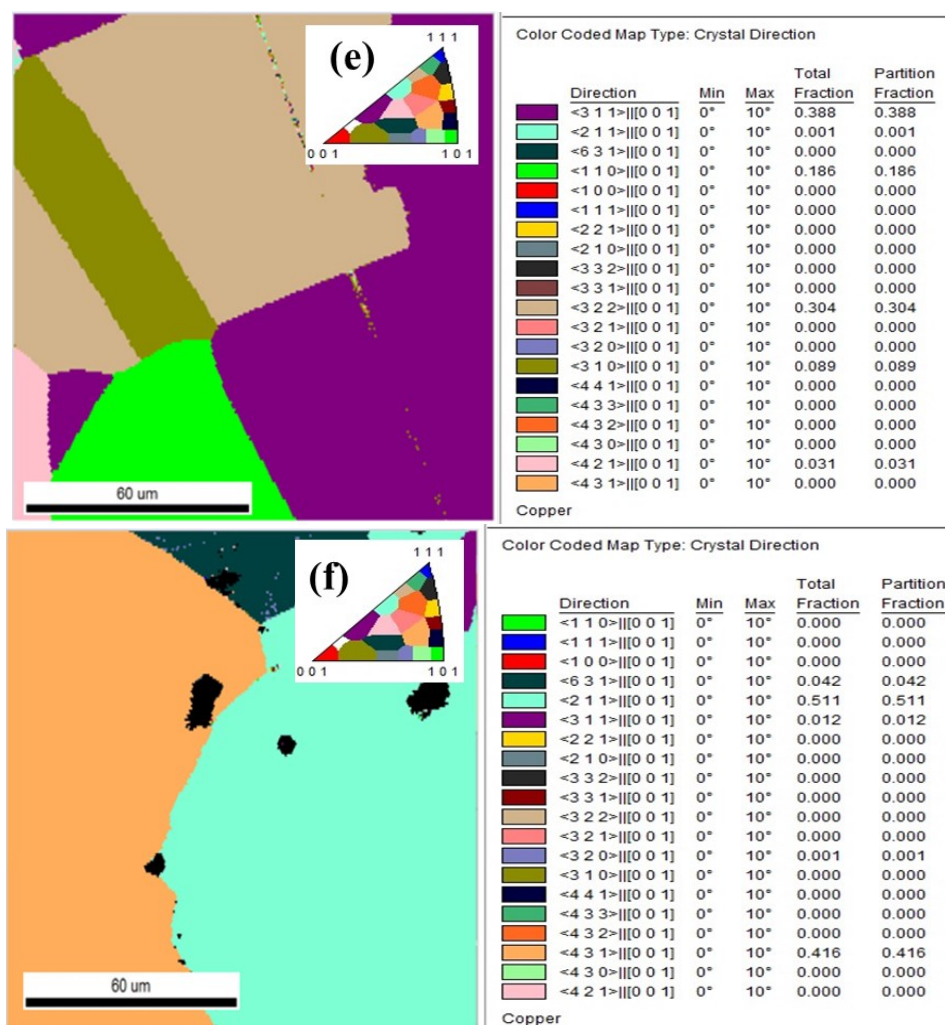


Fig. S5. Crystal orientation of as-prepared electrodes. (a) P-P-Cu, (b) P-Cu-200, (c) P-Cu-400, (d) P-Cu-600, (e) P-Cu-800, and (f) P-Cu-1000. Scale bar: 60 μm .

Table S1. Data for total grain boundaries distributions

S/No.	Catalyst	Total Grain Boundaries
1	P-P-Cu	65168
2	P-Cu-200	54005
3	P-Cu-400	15043
4	P-Cu-600	10227
5	P-Cu-800	3833
6	P-Cu-1000	2402

Table S2. Data for grain size variation across the electrodes in microns.

S/No.	Catalysts	Average Grain Size at 5° Tolerance Angle	Standard Deviation at 5° Tolerance Angle	Average Grain Size at 15° Tolerance Angle	Standard Deviation at 15° Tolerance Angle
1	P-P-Cu	4.66	4.48	4.64	4.76
2	P-Cu-200	4.64	4.25	4.70	4.54
3	P-Cu-400	7.58	8.61	7.72	8.90
4	P-Cu-600	11.01	15.96	10.82	16.55
5	P-Cu-800	17.91	28.92	17.27	28.53
6	P-Cu-1000	42.75	44.87	34.41	43.30

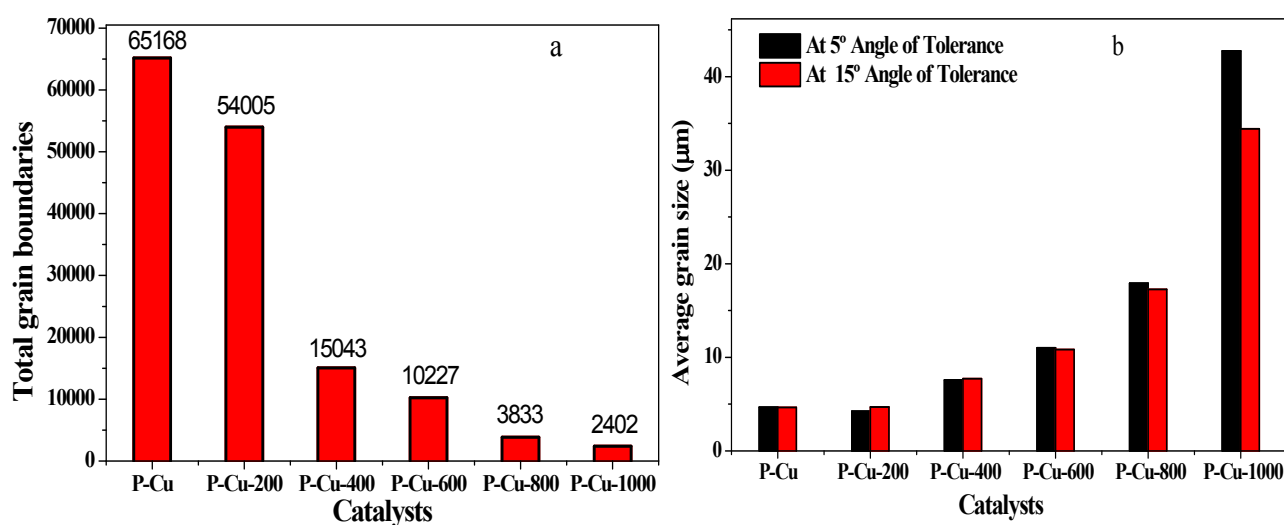


Fig. S6 a) Total grain boundaries distribution across different electrodes, and b) Grain size variation across different electrodes at 5° and 15° angle of tolerance.

Electrochemical CO₂ Reduction

The electrochemical CO₂ reduction reaction (CO₂RR) was performed in a three-electrodes-one-compartment reactor containing a 50 mL solution of 0.1 M KHCO₃ solution (pH 8.5) with Pt counter electrode and Ag/AgCl as the Reference electrode. 1.5 cm x 1.3 cm of the working electrode was dipped in the electrolyte during the CO₂RR. The electrolyte was vacuumed three times to remove dissolved gasses and then purged continuously with CO₂ for 30 minutes before each experiment to attain CO₂ saturated electrolyte. The CO₂RR was carried out in the CO₂-Saturated 0.1 M KHCO₃ (pH 6.8) solution at a constant bias of -1.0 V vs RHE, applied to the cathode using an electrochemical workstation (CHI 660D) over 4 hours period after which the current was measured as a function of time. During the CO₂RR process, the products in the gas phase (i.e. H₂, CO, and CH₄) were quantified with a gas chromatography-mass spectrometer (SHIMADZU, GCMS-DP2020) equipped with a barrier discharge ionization detector (BID-2010 plus) at every one hour for the Cu working electrodes. Ultrahigh purity helium (99.999%) was used as the carrier gas. However, this system cannot detect multicarbon gaseous products, such as C₂H₄.

After 4 hours of CO₂RR, the liquid products were detected by measuring out 665 μL of the electrolyte solution and mixed with 70 μL of 5 mM DMSO solution prepared in D₂O in glass vile and transferred into an NMR tube for NMR measurement. To determine the liquid product, ¹HNMR measurement was conducted using Bruker 400MHz NMR Spectrometer (Avance III) with water suppression. The product was elucidated using the MestReNova software.

The liquid products were quantified using the relative method which is based on standard calibration curve as reported elsewhere.¹⁻³ The standard concentration of formate and methanol were prepared and analyzed using the same instrument mentioned above. The Standard calibration curves (**Fig. S4**) were plotted from which the concentration of the liquid product was obtained. **Fig. S5** shows the NMR spectrum of a liquid product obtained from electrolyte collected after CO₂RR for each of our electrodes. We also performed blank measurements, where we only analyze the

electrolyte solution without any performing electrolysis, in order to ascertain if our product is actually the result of the electrolysis or the result of contaminations. The blank solution which is made up of 0.1 M KHCO₃ was prepared in the same way as the ones after electrolysis i.e., by mixing 665 μL of 0.1 M KHCO₃ with 70 μL of 5 mM DMSO solution prepared in D₂O. For the blank solution NMR measurement, we obtained 2 singlet peaks around the DMSO peak around 2.79 ppm and 2.44 ppm, which correspond to the Dimethylformamide (DMF) and Dimethylacetamide (DMA), respectively (Fig. S5a).⁴ These two peaks continued to appear around DMSO peak region during the analysis of the electrolytes after electrolysis on the electrodes, suggesting that these two peaks at 2.79 and 2.44 belong to the impurities from the as-prepared electrolyte solution. These measurements were conducted at room temperature. In addition to the gaseous product detected (H₂, CO, and CH₄), we also observed a singlet at 8.33 ppm corresponding to formate and another singlet at 3.23 ppm corresponding to methanol for the solutions collected after CO₂RR (See **Table S3**, and **Fig. S6**), although Methanol was not observed in P-Cu-600, P-Cu-800, and P-Cu-1000 solution.

Faradaic efficiency (FE)

This is the fraction of electricity driving the formation of a particular product during steady-state electrolysis. It represents the selectivity of the products during the CO₂RR process.

In this study, the faradaic efficiency was calculated by the following equations (eqn. 1 for the liquid product⁵ and eqn. 2 for gaseous products⁶):

$$FE_x = \frac{(c_p \times V_{cell} \times n_p \times F)}{Q_{Total}} \quad (1)$$

$$FE_x = \frac{(c_p \times n_p \times F)}{Q_{Total}} \quad (2)$$

c_p = concentration of product (in mol)

n_p = number of electrons transferred to reduce CO_2 to product (x)

F = Faradaic Constant (96485 Cmol^{-1})

Q_{total} = Total Charge (in C) obtained by integrating all the current (A) and the corresponding time (secs.).

V_{cell} = the electrolyte volume in the electrochemical cell in L

Current Density

This is calculated by dividing the total current by the geometric or total surface area of the electrode that was dipped into the electrolyte solution ($1.5 \text{ cm} \times 1.3 \text{ cm} = 1.95 \text{ cm}^2$). It also represents the total current density for the CO_2RR . There is a significant relationship between the total current density with the rate of CO_2 transformation. It is a key indicator of the cell's performance.

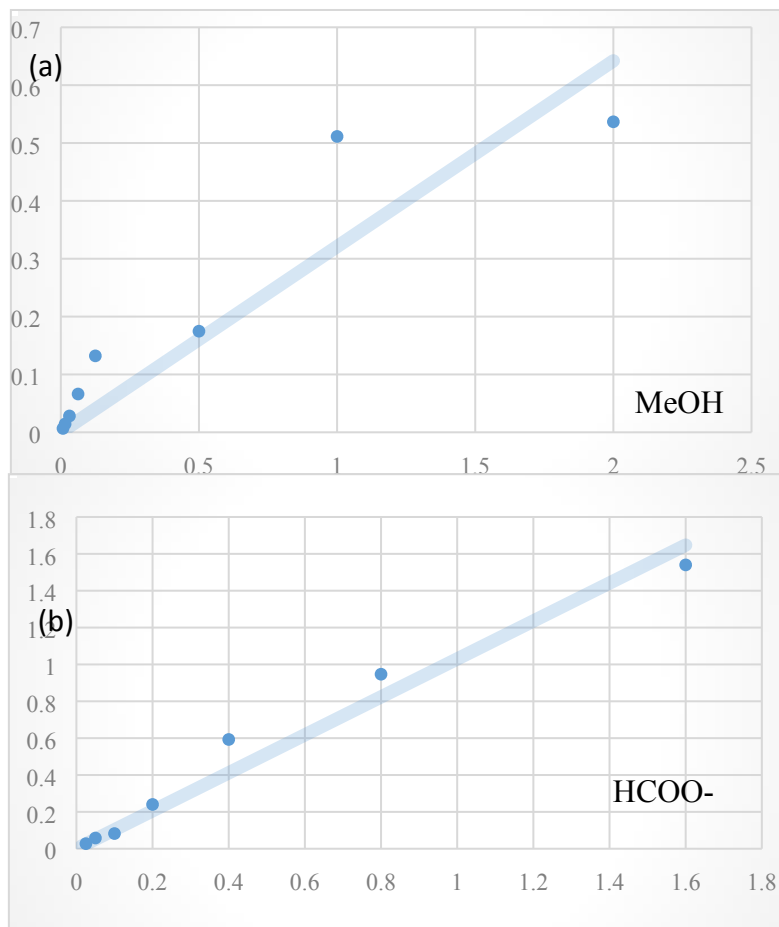
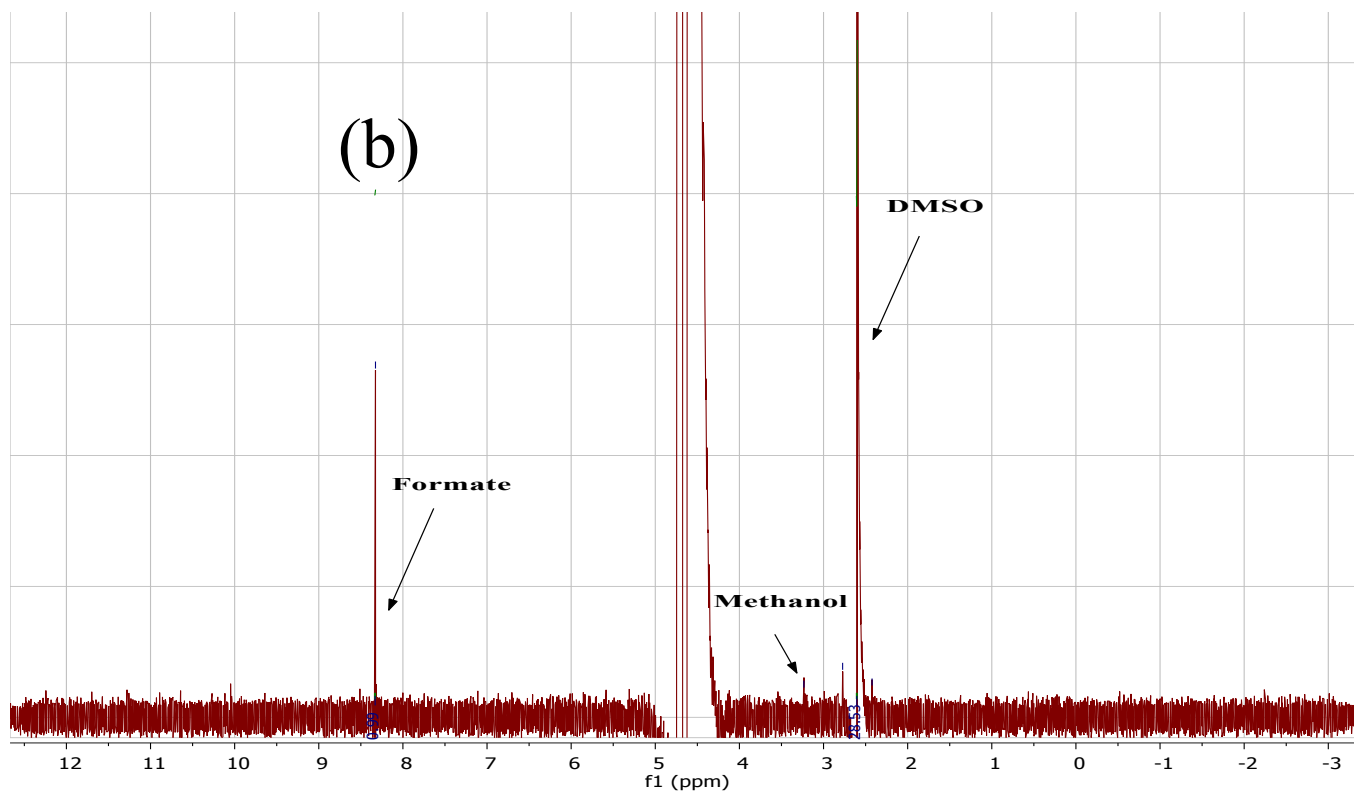
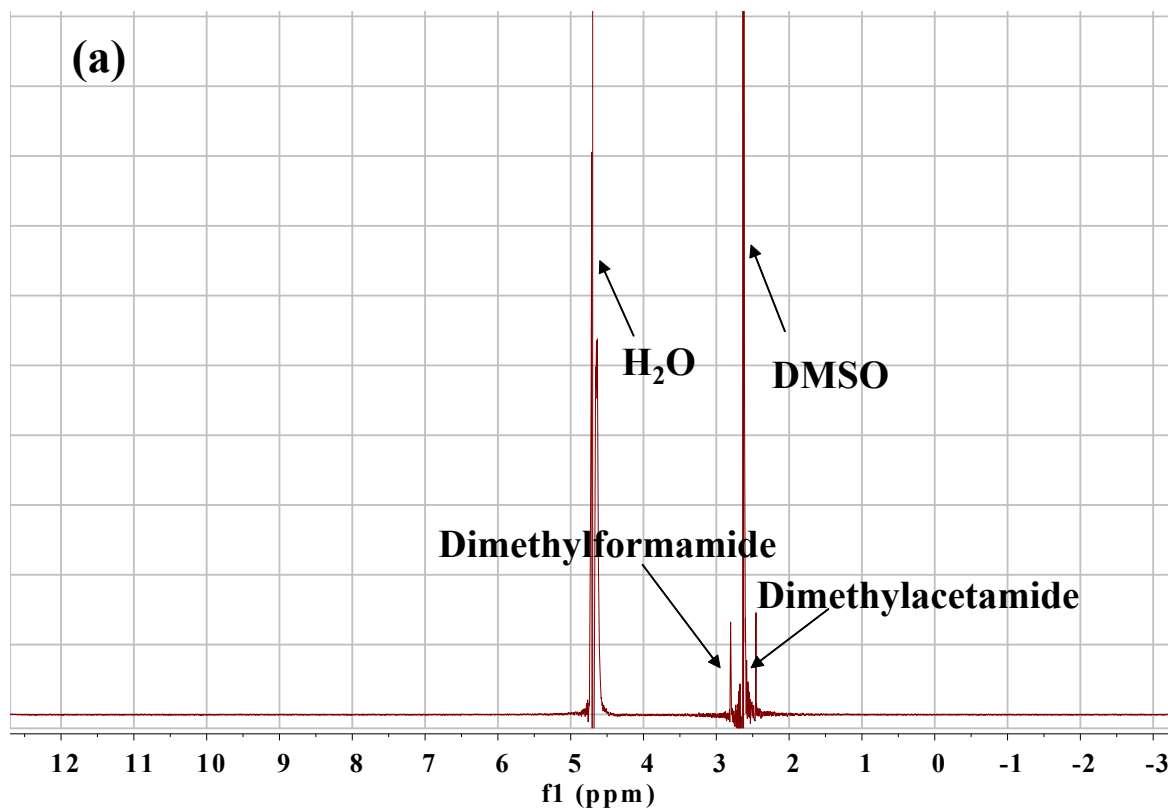
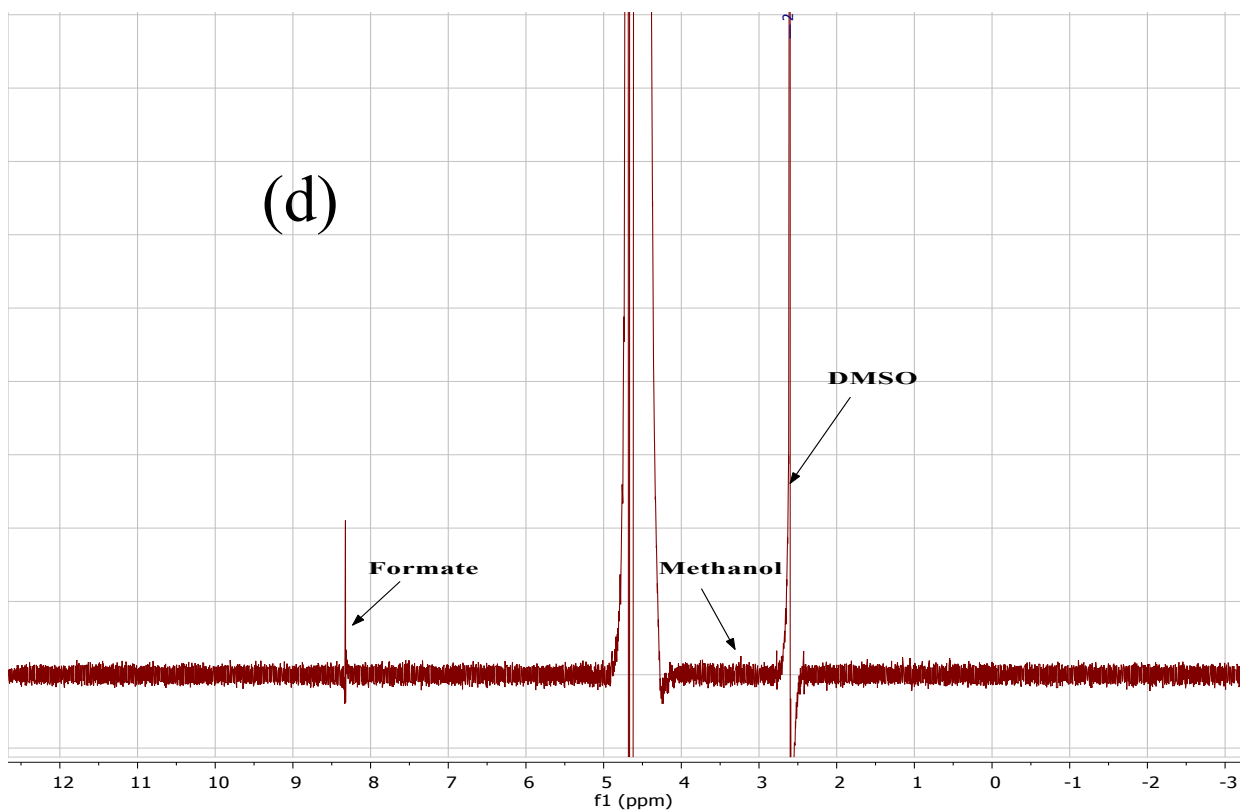
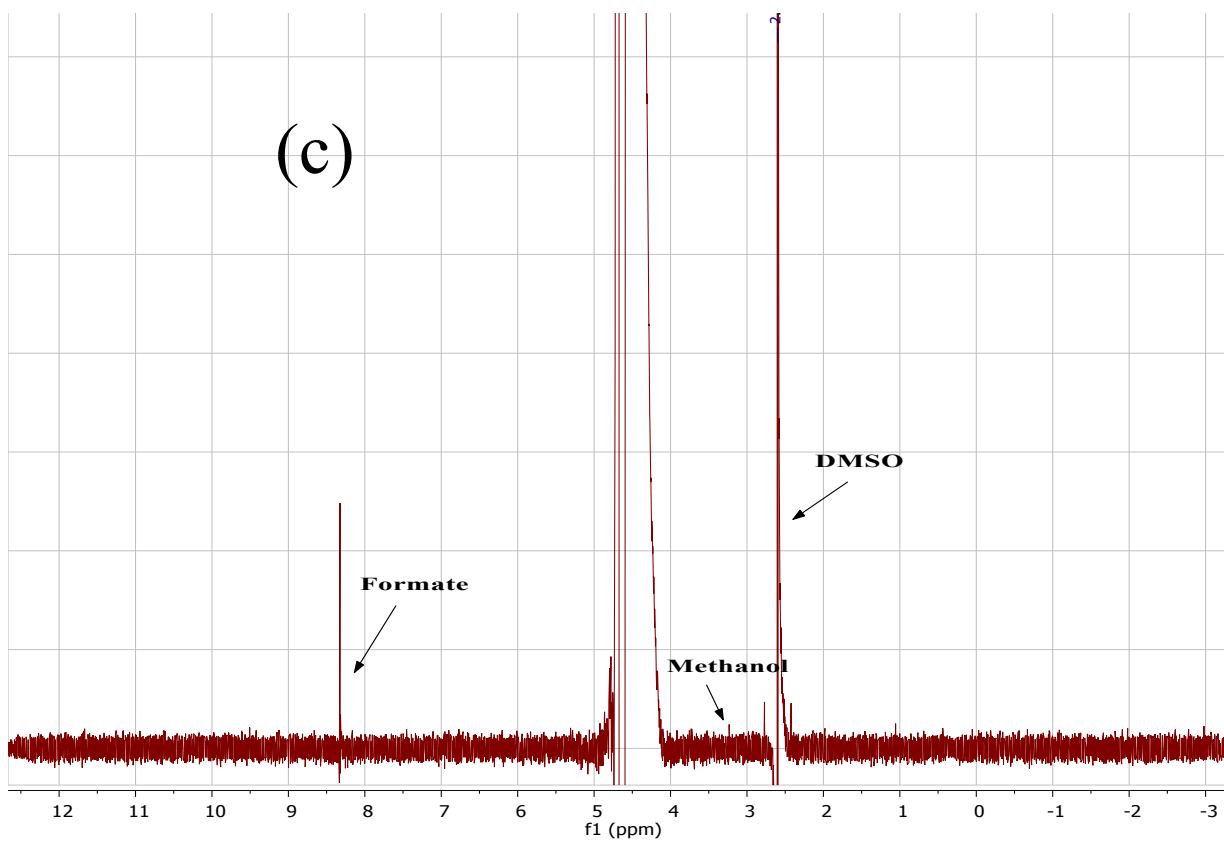
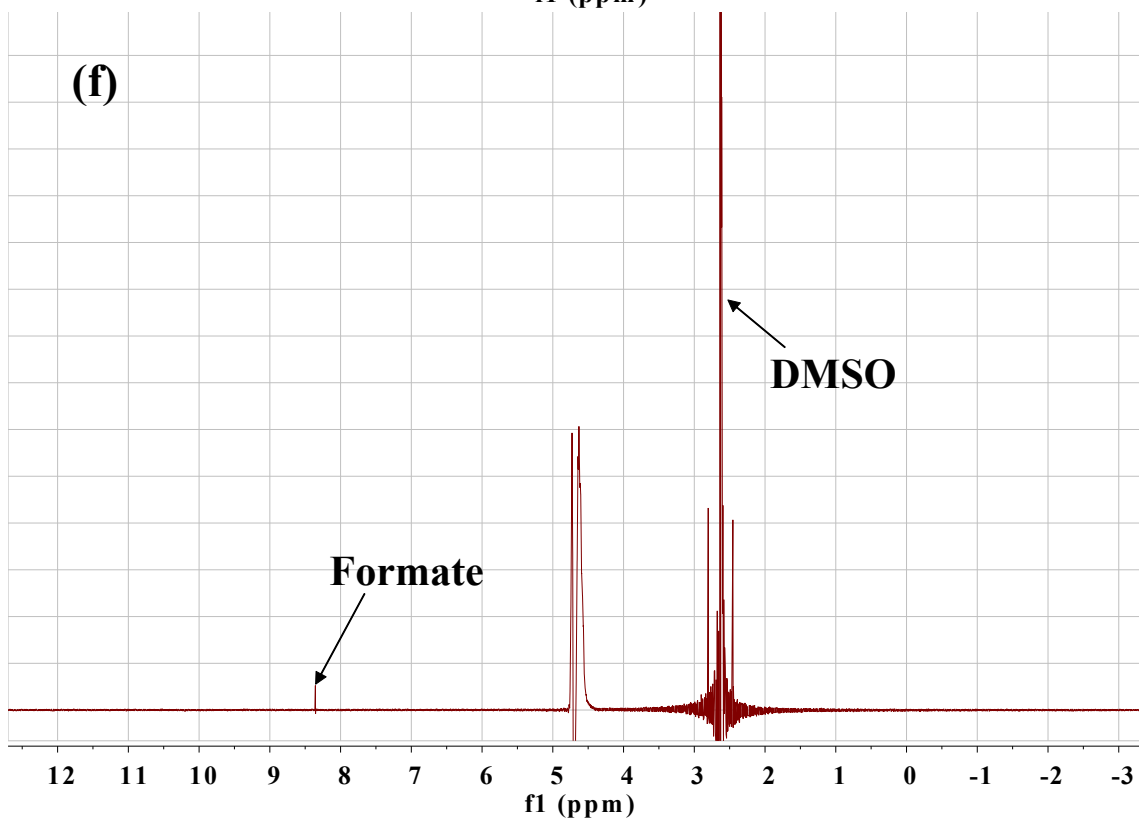
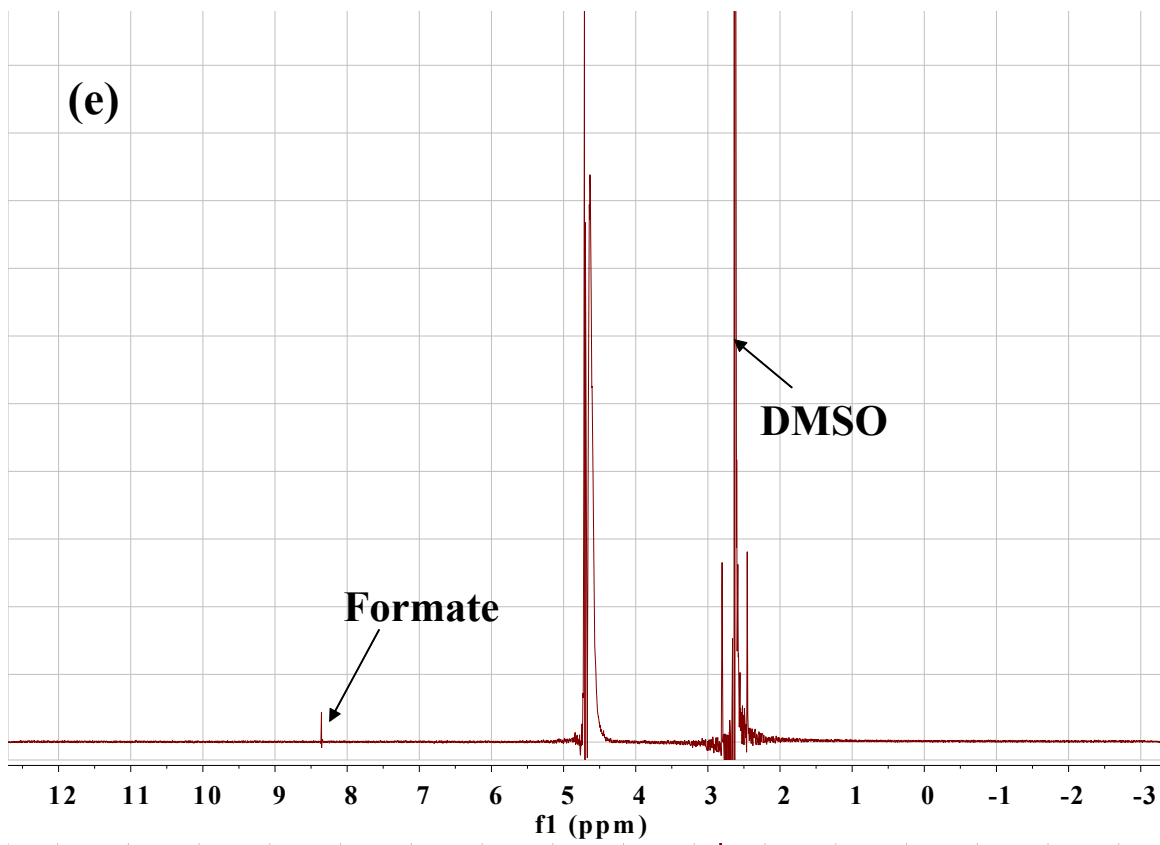


Fig. S7 Standard calibration curves: (a) MeOH and (b) HCOO⁻.







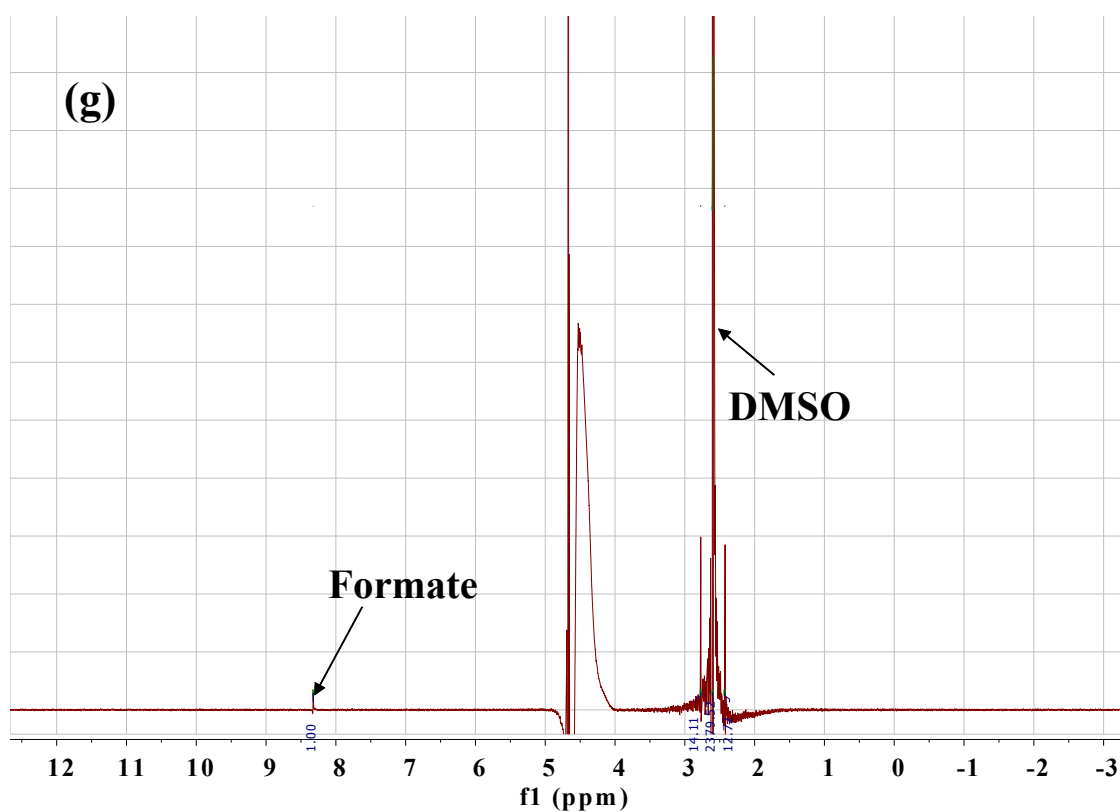


Fig. S8 NMR spectra of liquid products: a) blank, b) P-Cu, c) P-Cu-200, d) P-Cu-400, e) P-Cu-600, f) P-Cu-800, and g) P-Cu-1000.

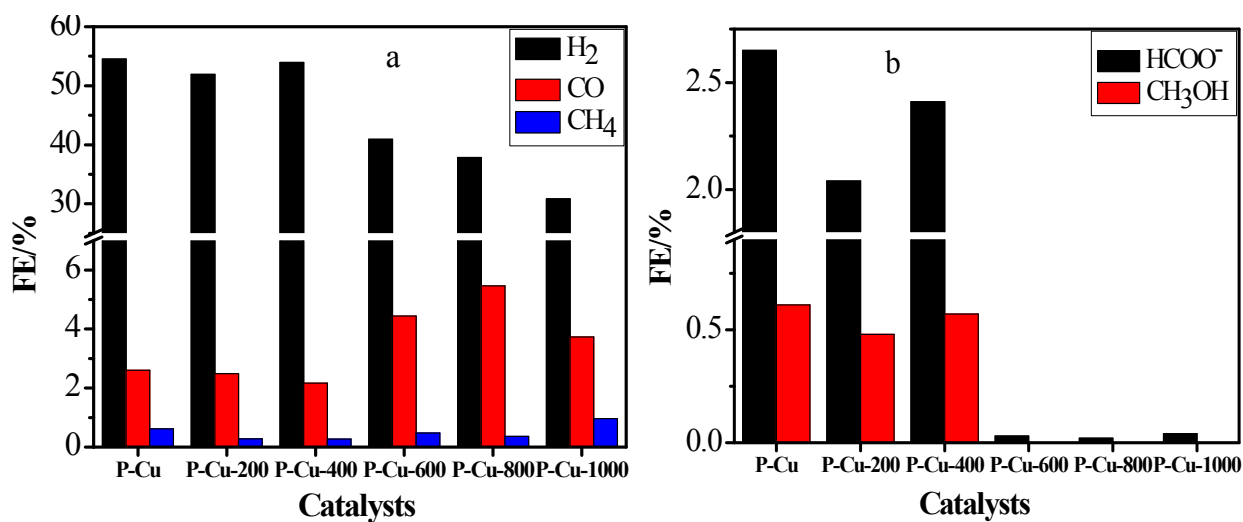


Fig. S9 Faradaic efficiency of a) gaseous and b) liquid products over the different Cu electrodes at -1.0 V vs RHE quantified after 4 h electrolysis.

Table S3. Product rate ($\mu\text{mol cm}^{-2}\text{ h}^{-1}$) (ND= Not Detected)

Catalyst	H ₂	CO	CH ₄	HCOO ⁻	CH ₃ OH
P-P-Cu	34.23	1.63	0.097	25.58	2.27
P-Cu-200	31.64	1.52	0.040	23.69	2.99
P-Cu-400	25.71	1.03	0.032	22.92	1.81
P-Cu-600	17.15	1.86	0.050	0.27	ND
P-Cu-800	13.55	1.95	0.064	0.17	ND
P-Cu-1000	11.47	1.39	0.090	0.31	ND

Table S4. Yield ($\mu\text{mol cm}^{-2}$) and Faradaic efficiencies over selected Cu electrodes (ND= Not Detected)

Catalyst	H ₂		CO		CH ₄		HCOO ⁻		CH ₃ OH	
	Yield	FE	Yield	FE	Yield	FE	Yield	FE	Yield	FE
P-P-Cu	234.5±3	54.33±	11.9±0.	2.79±0	0.6±0.	0.54±0	198.7±	2.35±	16.45±1	0.58±
	2.54	0.2	84	.19	17	.08	0.8	0.31	.25	0.04
P-Cu-200	242.32±	53.25±	11.62±	2.56±0	0.35±0	0.31±0	171.88	1.89±	18.91±4	0.63±
	4.5	1.25	0.23	.07	.04	.03	±12.88	0.15	.39	0.15
P-Cu-800	104.26±	35.54±	21.42±	7.2±1.	0.43±0	0.41±0	2.16±0	0.03±	ND	ND
	1.46	2.31	6.18	74	.07	.05	.31	0.01		
P-Cu-1000	71.79±1	24.41±	8.28±2.	2.07±0	0.78±0	0.79±0	2.5±0.	0.04±	ND	ND
	7.65	6.41	55	.19	.08	.07	05	0.0		

References

- 1 D. Raciti, K. J. Livi and C. Wang, *Nano. Lett.* 2015, **15**, 6829–6835.
- 2 K. P. Kuhl, E. R. Cave, D. N. Abram, and T. F. Jaramillo, *Energy Environ. Sci.* 2012, **5**, 7050–7059.
- 3 U. Holzgrabe, *Prog. Nucl. Magn. Reson. Spectrosc.* 2010, **57**, 229–240.
- 4 G. R. Fulmer, A. J. M. Miller, N. H. Sherden, H. E. Gottlieb, A. Nudelman, B. M. Stoltz, J. E. Bercaw, K. I. Goldberg, R. Gan and H. Apiezon, *Organometallics* 2010, **29**, 2176–2179.